J. Cell. Mol. Med. Vol 12, No 1, 2008 pp. 209-218

Pleomorphism of the nuclear envelope in breast cancer: a new approach to an old problem

Gianni Bussolati *, Caterina Marchiò, Laura Gaetano, Rosanna Lupo, Anna Sapino

Department of Biomedical Science and Human Oncology, University of Torino, Via Santena, Torino, Italy

Received: July 23, 2007; Accepted: October 16, 2007

Abstract

In routine practice, nuclear pleomorphism of tumours is assessed by haematoxylin staining of the membrane-bound heterochromatin. However, decoration of the nuclear envelope (NE) through the immunofluorescence staining of NE proteins such as lamin B and emerin can provide a more objective appreciation of the nuclear shape. In breast cancer, nuclear pleomorphism is one of the least reproducible parameters to score histological grade, thus we sought to use NE proteins to improve the reproducibility of nuclear grading. First, immunofluorescence staining of NE as well as confocal microscopy and three-dimensional reconstruction of nuclei in cultured cells showed a smooth and uniform NE of normal breast epithelium in contrast to an irregular foldings of the membrane and the presence of deep invaginations leading to the formation of an intranuclear scaffold of NE-bound tubules in breast cancer cells. Following the above methods and criteria, we recorded the degree of NE pleomorphism (NEP) in a series of 273 invasive breast cancers tested by immunofluorescence. A uniform nuclear shape with few irregularities (low NEP) was observed in 135 cases or, alternatively, marked folds of the NE and an intranuclear tubular scaffold (high NEP cases) were observed in 138 cases. The latter features were significantly correlated (*P*-value <0.002) with lymph node metastases in 54 histological grade 1 and in 173 cancers with low mitotic count. Decoration of the NE might thus be regarded as a novel diagnostic parameter to define the grade of malignancy, which parallels and enhances that provided by routine histological procedures.

Keywords: pleomorphism • nuclear envelope • immunofluorescence • breast cancer

Introduction

Irregularities in both nuclear shape and size ('pleomorphism'), coupled with changes in chromatin amount and distribution, remain the basic microscopic criteria for a cytologic diagnosis of cancer. Moreover, in several cancer types (*e.g.* in breast cancer), nuclear pleomorphism is graded and correlates with clinical aggressiveness and patient outcome [1, 2]. Despite the widespread use of such morphological criteria for the daily cytological diagnoses on smears and fine-needle aspiration biopsies (FNA), it should be acknowledged that the light microscopy appreciation of nuclear pleomorphism is currently indirect, being based on staining of nucleic acids with basic dyes such as haematoxylin. Since heterochromatin is strictly bound to the nuclear membrane, we can derive indirect information on heterochromatin distribution using routine nuclear stains. As a result,

*Correspondence to: Professor Gianni BUSSOLATI, Department of Biomedical Science and Human Oncology, University of Torino, Via Santena 7, 10126 Torino, Italy.
Tel.: +39-011-6334274
Fax: +39-0116635267
E-mail: gianni.bussolati@unito.it

doi: 10.1111/j.1582-4934.2007.00176.x

consistency in classification of nuclear grade (NG) in general and specifically in breast cancer by haematoxylin and eosin is less than optimal, as the agreement of even expert pathologists ranges from 0.35 [3] to 0.59 [4] by kappa statistics.

Indeed, indentations, undulations and folds of the nuclear membrane, as originally reported by ultrastructural observations [5], occur early in neoplastic processes and are detectable even in the pre-cancerous stage [6], and mark a difference from the smooth, roundish nuclear shape of the normal cells of corresponding tissues and organs [7]. The deep biological significance of nuclear pleomorphism has been confirmed by *in vitro* models, which demonstrated that induced gene mutations are associated to tumour-specific nuclear changes. In thyroid cancer, for example, it has been shown that micro-injection of the RET/PTC oncogene into thyroid cells, leading to the activation of a tyrosine kinase, is able to induce nuclear envelope (NE) irregularity within hours, without a requirement for a post-mitotic NE reassembly [8–10].

Progress in the analysis of the NE revealed the presence of several components: nuclear lamina, inner nuclear membrane, outer nuclear membrane, nuclear pore complexes and statin, a non-proliferation nuclear-specific protein [11–15]. Lamin B, a structural component of the lamina, marks the proteinaceous layer at the interface between chromatin and the inner nuclear membrane, emerin is a trans-membrane protein crossing both the inner and the outer membranes [16, 17] and nucleoporin is associated with nuclear pores (the discontinuous complexes joining the inner and outer membrane) [18, 19]. In a previous study we showed that immunofluorescent decoration of NE with anti-lamin B antibodies followed by three-dimensional (3D) reconstruction of confocal microscopic images allowed appreciation of fine arrangements of the nuclear shape in papillary thyroid carcinoma [20].

We have now expanded this approach to breast cancer with the final aim to evaluate whether appropriate markers of the NE and tracing of NE-associated proteins might yield a more objective and direct appreciation of nuclear pleomorphism of cancer cells.

Materials and methods

Cell lines

Breast cancer cell lines MCF7, BT474 and SKBR3 were obtained from the American Type Culture Collection (Manassas, VA, USA). Cells were grown in IDMEM (Iscove Dulbecco's Modified Eagle's medium) (Sigma Aldrich, St. Louis, MO, USA) supplemented with 10% foetal calf serum (Seromed, Berlin, Germany), 2 mmol/l glutamine, 100 U/ml penicillin and 100 μg/ml streptomycin (all from Sigma), and incubated at 37°C, 5% CO_2.

Primary cultures of breast epithelium were obtained from reduction mammoplasties [21]. Tissues were digested with collagenase IA 200 U/ml and hyaluronidase 100 U/ml (all from Sigma). Purification was then completed following the Dynabeads Magnetic Separation method (Dybal Biothec, Oslo, Norway). Cells were grown in DMEM/Ham's F12 (Dulbecco's Modified Eagle's medium, Sigma) supplemented with 10% foetal calf serum (Seromed), 0.01 mg/ml insulin, 500 ng/ml hydrocortisone and 20 ng/ml Epidermal Growth Factor (all from Sigma).

For immunofluorescence (IF) staining, cells were plated on multi-chamber slides (Becton Dickinson, San Jose, CA, USA) and cultured in Iscove – Dulbecco's Modified Eagle's medium (IDMEM) until a 70% cellular confluence was reached. Cells were then fixed in methanol for 5 min. at –20°C and permeabilized in acetone for 5 sec. at –20°C, then brought to phosphate-buffered saline (PBS).

Histological specimens

A preliminary investigation was conducted in five cases of histologically normal breast tissue and five cases of invasive breast cancer. Additionally, a series of consecutive 304 cases of unifocal invasive breast cancer, processed following the tissue micro array procedure as outlined by Sapino *et al.* [22] were included in the study. The NG of such cases had originally been established according to Elston and Ellis [1]. Briefly, for each case, the selection of at least four fields was carried out on the original haematoxylin and eosin stained slides during assessment of the histological grade, in order to guarantee that the most significant intratumoral variations in terms of tubular formation, nuclear atypia and mitosis number were identified. The number of selected fields varied from 4 to 6 depending on the heterogeneity both of the histological pattern and of the grade of differentiation of the invasive breast cancer component.

Four micrometre thick sections of the paraffin block were collected onto poly-L-lysine coated slides. Sections were dehydrated in graded alcohols and processed for IF. Marked and diffuse irregularities of the nuclear membrane leading to the building up of a scaffold of intranuclear foldings were classified as high NEP, while mild-to-moderate NE irregularities with rare or absent intranuclear invaginations were classified as low NEP (Table 1). Classification of cases into either high or low NEP categories was independently determined by the two senior authors blinded to the original histological grade. Cases were evaluated as tissue arrays and in each case 4 core, representative of different tumour foci, were selected. As a rule (in more

Table 1 Nuclear envelope pleomorphism (NEP) categories as defined by immunofluorescence and nuclear grade (NG) score values as defined by haematoxylin and eosin.

NEP	
Low	Mild or moderate NE irregularities, with rare or absent strands or intranuclear invaginations (see Figs 2A and 4B)
High	Marked irregularities of the nuclear membrane and frequent strands or intranuclear invaginations (see Figs 2C and 3A)
NG*	
Score 1	Nuclei small with little increase in size in comparison with normal breast epithelial cells, regular outlines, uniform nuclear chromatin, little variation in size
Score 2	Cells larger than normal with open vesicular nuclei, visible nucleoli and moderate variability in both size and shape
Score 3	Vesicular nuclei, often with prominent nucleoli, exhibiting marked variation in size and shape, occasionally with very large and bizarre forms

*Reference [7].

Table 2 Antibodies anti-nuclear envelope (NE).

Primary antibody	Dilution in PBS-BSA	Antigen retrieval for FFPE† tissues	Secondary antibody	Dilution in PBS-BSA
Goat anti-lamin B (SC-6217; Santa Cruz, CA, USA)	1:5	Microwave 10 min. in citrate buffer (pH 6) at 98°C	Fluorescein isothiocyanate-conjugated rabbit anti-goat (Sigma Aldrich, Munich, Germany)	1/200
Rabbit anti-emerin (ab14208; Abcam, Cambridge, UK)	1/500	Microwave 40 min. in citrate buffer (pH 6) at 98°C	Rhodamine isothiocyanate-conjugated swine anti-rabbit (DAKO, Glostrup, Denmark)	1/300
Mouse anti-nucleoporin* (ab 24700; Abcam)	1/200		Fluorescein isothiocyanate-conjugated goat antimouse (Sigma)	1/100

†FFPE: formalin fixed paraffin embedded.
* Not tested on FFPE.

than 80% of the cases) the nuclear shape was similar and homogeneous (either low or high NEP) in all cores of each case. In case of variability within different cores of the same case the high NEP category was assigned, whereas inter-observer discrepancies, which occurred in 21 cases, were solved by consensus. We can roughly reckon that each core (diameter 1 mm) was presenting approximately 1000 cancer cells. More than 50% of cancer nuclei had to present a high grade of NE pleomorphism in order the case to be considered as high NEP.

Immunofluorescence

Cells and histological slides were immunostained for NE evaluation (Table 2). Cells and tissues were treated with a blocking serum (Mabtech AB, Germany), diluted 1/100, for 30 min. at room temperature and then incubated with the primary antibody for 1 hr. The slides were then rinsed three times in PBS and incubated for 45 min. with the specific secondary antibody. Finally, the slides were rinsed three times with PBS prior to mounting with an anti-fading

mounting medium (VECTASHIELD® Mounting Medium, Vector Laboratories, Burlingame, CA, USA).

Images acquisition

Tissue sections were examined with an Olympus BX51 fluorescence microscope (Olympus, Hamburg, Germany) and images were acquired using an Olympus C-7070 wide zoom camera. For confocal scanning laser microscopy, we alternatively used a LSM5 PASCAL confocal microscope (Carl Zeiss, Germany) or a FV300 confocal microscope mounted on an IX71 inverted microscope (both from Olympus), or a TCS SP2 confocal microscope (Leica, Wetzlar, Germany). Areas of non-overlapping nuclei were selected for scanning at 63× magnification. Serial sections were recorded with a 0.3 μm gap between sections.

3D reconstruction

Using the serial images obtained by confocal microscopy, 3D models of selected nuclei were obtained employing Amira 4.0, advanced 3D visualization and volume modelling software (TGS Template Graphics Software, http://www.tgs.com). Briefly, using sequential images of serial nuclear sections, segmentation of the region of interest was obtained outlining the nuclear profile. Each segment of the curve matching the steps between sections was proportional to the size of the nuclei and to the gaps between sections, as measured by confocal microscopy. The segmented areas were then exploited to generate 3D polygonal surface models.

Statistical analysis

The following parameters were analysed on the series of breast cancers: nuclear envelope pleomorphism (NEP) as revealed by IF, score values of NG as defined by haematoxylin and eosin (Table 1) and histological grade (G). Marked and diffuse irregularities of the nuclear membrane leading to the building up of a scaffold of intranuclear foldings were classified as high NEP, while mild to moderate NE irregularities with rare or absent intranuclear invaginations were classified as low NEP (Table 1). Association between NEP and NG or G were evaluated. The correlation between NEP and the lymph node status and prognostic parameters, such as oestrogen and progesterone receptors, Ki67 and Her2 values, was analysed using the chi-square test and logistic regression analysis (Table 3).

Statistical analysis was performed by STATISTICA 7 software (StatSoft Inc., USA).

Results

Lamin B, emerin and nucleoporin shared a similar distribution in the nuclear membrane, as also confirmed by dual IF staining. Lamin B and emerin revealed a continuous layer (Fig. 1), while nucleoporin expression was more granular and discontinuous.

NE morphology in cell cultures

In primary cultures of normal mammary epithelium a uniform shape with an even NE edge was commonly observed (Fig. 2A). Only occasional, scanty irregularities or isolated intranuclear foldings were detected. On the other hand, irregularities of the nuclear contour, shaping indentations and foldings of the NE were common features of all three breast cancer cell lines examined. In most cancer cells, linear strands or digitations protruding from the surface deep into nucleus were observed. Such intranuclear strands, best revealed by lamin B or emerin decoration, varied in number with some cells showing as many as four or more in the same nucleus (Fig. 2C).

3D reconstruction of NE in cell culture

3D models of the nuclei of normal cells showed oval to ellipsoidal structures with a very smooth surface and rare indentations (Fig. 2B). In cancer cells, 3D reconstruction allowed the building up of proper models and appreciation of the deep invaginations and tubular structures entering the nuclei (Fig. 2D). On single images obtained by confocal microscopy, intranuclear digitations appeared as intranuclear spots, while upon 3D reconstruction they invariably connected to the outer membrane. Using the Amira software, the total extension of the NE was measured both in breast cancer cells and in normal mammary cells (from primary cultures). The ratio obtained between nuclear surface of cancer cells and normal cells demonstrated a marked increase in nuclear surface proper of the former, *i.e.* the ratio of the surface extension of nuclei of MCF7 breast cancer cells as

Table 3 Correlations between NEP and other clinical and histopathological parameters: ER (+ *versus* –), PgR (+ *versus* –) HER2 (+ *versus* –), Ki67 (> *versus* < 20%), pN (No *versus* N1) and pT (T1 *versus* T > 1), as established by chi-square analysis.

	LNEP	HNEP	P-value
ER			
–	22 (16%)	18 (13%)	0.556
+	113 (84%)	120 (87%)	
PgR			
–	43 (32%)	35 (25%)	0.292
+	92 (68%)	103 (75%)	
HER2			
–	119 (88%)	119 (86%)	0.770
+	16 (12%)	19 (14%)	
Ki67			
–	69 (51%)	73 (53%)	0.861
+	66 (49%)	65 (47%)	
PN			
N0	81 (60%)	63 (46%)	0.024
N1	54 (40%)	75 (54%)	
PT			
T1	83 (61%)	56 (41%)	0.001
T > 1	52 (39%)	82 (59%)	

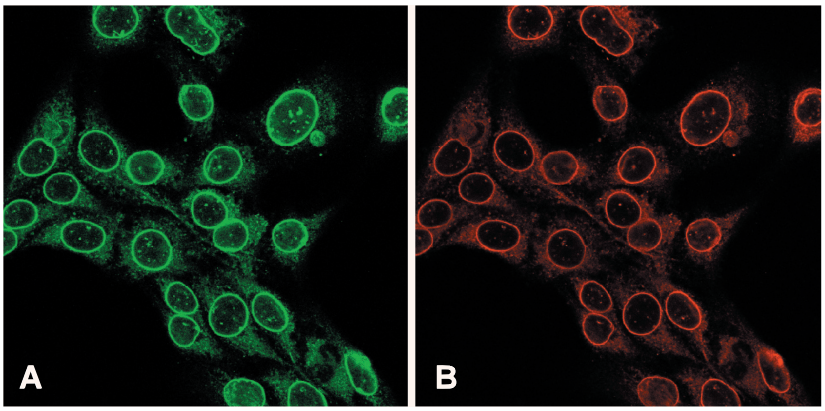

Fig. 1 SKBr3 breast cancer cell line, stained with (**A**) anti-lamin B antibodies (revealed with fluorescein) and (**B**) anti-emerin antibodies (revealed with rhodamin). The two proteins linked to the nuclear membrane share a similar distribution, not only at the nuclear surface, but in intranuclear deposits as well.

related to that of normal mammary epithelial cells was in the range of 2.4.

NE morphology in tissue specimens and correlation with lymph node metastases

On tissue sections, restaining of the IF preparations with haematoxylin and eosin showed the superior information provided by the IF tracing of NE proteins and how nuclear indentations and invaginations were not or only minimally recognizable by the heterochromatin staining provided by haematoxylin (Fig. 3A and B). IF analysis of normal epithelium showed a regular shape with a smooth profile, while fine undulations of the NE were observed in the basally located myoepithelial cells (Fig. 3C and D).

IF analysis was successfully recorded in 273 of 304 breast cancers tested, because cases with cracked cores or less than three cores available after IF staining were not considered for NEP evaluation. Approximately half of the cases were classified as high NEP and the remaining with low NEP. The association between NEP and NG or G or other biological and prognostic factors was not statistically significant

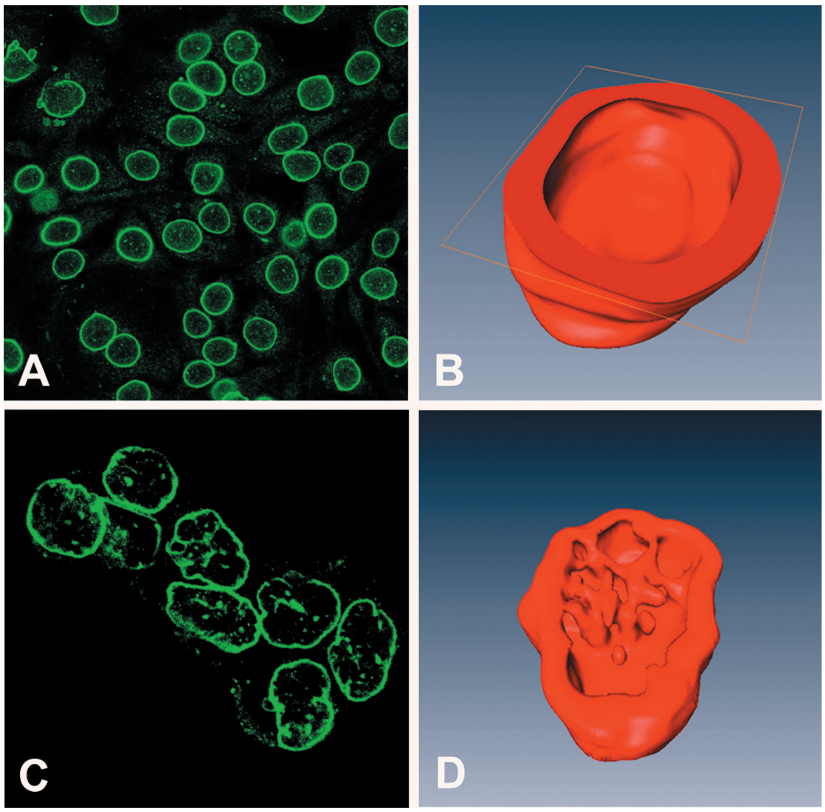

Fig. 2 The arrangement of the nuclear membrane, as revealed by tagging membrane-associated lamin B, was observed by confocal microscopy, in cells from primary cultures of normal mammary epithelium (**A**) and in BT474 breast cancer cells (**C**). The 3D reconstruction of the serial sections allows to appreciate the smooth roundish shape on 'normal' nuclei (**B**) as compared to the deep foldings and intranuclear tubules in cancer cells (**D**).

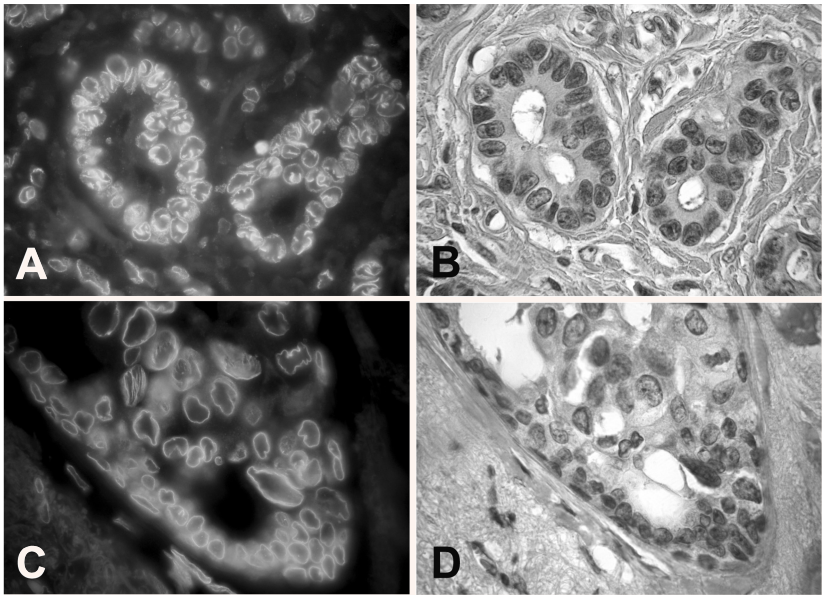

Fig. 3 IF staining with anti-emerin antibody outlined high NEP (**A**) in a histologically low-grade ductal carcinoma (G1) as shown by staining with haematoxylin and eosin of a parallel section (**B**). Anti-emerin antibody delineates the smooth profile of nuclei of normal residual epithelium (arrows) in a ductal high nuclear grade carcinoma *in situ* (**C**, **D**).

(Table 3 & 4) except for size (pT) and lymph node status (pN). We then investigated the role of NEP to predict lymph node metastases. Interestingly, the subclassification of well-differentiated G1 cancers in low NEP and high NEP significantly correlated with lymph node status (*P*-value 0.0003) (Table 5). In analogy, there was a significant difference (*P*-value 0.0016) between low NEP and high NEP in tumours

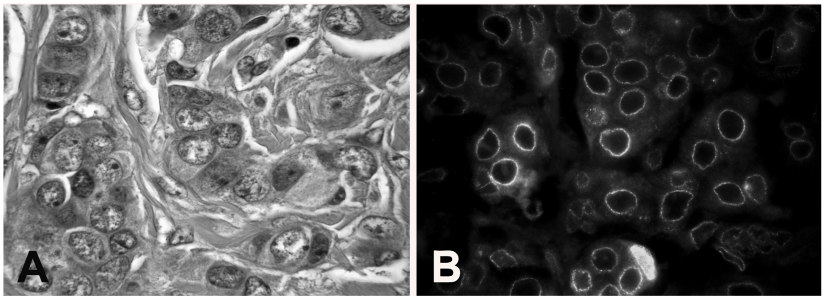

Fig. 4 Haematoxylin and eosin staining of G3 invasive carcinoma: the nuclei meet the criteria for score 3, being vesicular, with prominent nucleoli and exhibiting marked variation in size (**A**). NE staining with anti-emerin antibody in IF shows instead a smooth profile (**B**), corresponding to low NEP.

Table 4 Association between nuclear envelope pleomorphism (NEP) and histological grade (G) or nuclear grade (NG).

	Low NEP	High NEP	Chi-square test *P*-value
G			
G1/G2	89 (52%)	82 (48%)	0.27
G3	46 (45%)	56 (55%)	
NG			
NG1/NG2	89 (52%)	81 (48%)	0.22
NG3	46 (45%)	57 (55%)	

Table 5 Impact of nuclear envelope pleomorphism (NEP) on lymph node (LN) metastases in low histological grade (G1) and mitotic score 1 (from 0 to 8 mitoses per 10 fields in a microscopic field of 0.55 mm) tumours.

	LN metastases		Chi-square test
G	No	Yes	*P*-value
G			
Low NEP	32 (91%)	3 (9%)	0.0003
High NEP	9 (47%)	10 (53%)	
Mitotic count Score 1			
Low NEP	59 (72%)	23 (28%)	0.0016
High NEP	44 (48%)	47 (52%)	

with a mitoses score of 1 (from 0 to 8 mitoses per 10 fields of 0.55 mm) [23] (Table 5). The next step was to investigate the relative significance of NEP to predict lymph node metastases by logistic multiple regression. In the analysis of the whole series of breast cancers only the linear combination of tumour size (pT) and G contributed to explain the presence of metastases (R2 of 0.181), while the addition of NEP as the independent variables increased R2 to only 0.183. However, size lost its significance (*P*-value 0.856) in the subcategory of G1 tumours, while NEP represented the only variable that correlated significantly with lymph node metastases (*P*-value 0.001).

Discussion

Nuclear pleomorphism has long been known as a typical feature of cancer cells and still retains a fundamental role in daily cyto-histological diagnoses. In the present work we traced the NE of breast cancer cells directly by IF of proteins strictly linked to the nuclear membrane, such as lamin B and emerin [9, 16, 18]. Previous studies showed that lamins, whose function is to link heterochromatin domains to the inner nuclear membrane [24–26], are important mediators of nuclear shape. In fact, nuclear pleomorphism can be the result of genetic alteration leading to laminopathies [27]. IF investigations in cancer cells revealed localization of lamina proteins not only at the periphery, but well inside the nucleus [28]. Evidence of intranuclear membrane extensions had already been shown by electron microscopy in plant cells [29, 30] as well as in mammalian cells [31–33]. In a very extensive and well-documented study, Fricker *et al.* [34] were able to decorate such intranuclear tubular extensions in several mammalian cell lines and primary cultures giving evidence of them being a dynamic compartment spatially close to the nucleolus and favouring transport from the nucleus to the cytoplasm. More recently, intranuclear tubules were shown to be the site of Ca^{2+} release [35].

Our results in *in vitro* cultures showed that nuclei of 'normal' epithelium (from primary cultures) displayed an uniformly smooth silhouette, while in most breast cancer cell lines intranuclear deposits of lamin B and emerin were detected as spots which, upon

3D reconstruction, resulted to build up a scaffold. As allowed by Amira software, the ratio of total extension values of the NE, between breast cancer cells and normal mammary cells (from primary cultures) demonstrated a marked increase in nuclear surface proper of the former. It can thus be imagined that NE irregularities and intranuclear tubules might be involved in or be reactive to defects in the nuclear-cytoplasmic transport, reportedly a feature typical of cancer cells [36].

Still, despite their considerable biological interest, the intranuclear tubular extensions of the NE have not yet gained attention in pathology. In the seminal work by Elston and Ellis [1], which led to the modification of Bloom and Richardson histological grade in breast cancer, nuclear pleomorphism is assessed using three score values. These score values are given by comparing tumour nuclei with nuclei of normal breast and by considering at least four features: size, shape, uniformity of nuclear chromatin, nucleoli, so that score 1 nuclei are little larger, but very similar to normal cell nuclei, while score 3 nuclei show marked variation in size and a 'bizarre' morphology (Table 1). Yet, light microscopy appreciation of foldings and indentations of the nuclear membrane is rough and indirect, being based on the staining of membrane-bound heterochromatin. In the present work, we showed that high nuclear pleomorphism, as defined by staining of the NE proteins emerin and lamin, may recognize among histologically low-grade cancer (G1) and in tumours with low proliferation activity (mitotic count score 1), those more prone to metastasise to lymph node. Systematic differences between pathologists in scoring nuclear pleomorphism in breast cancer potentially contribute to differences in allocating overall grade and confirm the need for improved nuclear grading criteria [3, 4]. In addition, nuclear atypia, as traditionally evaluated by pathologists, has only limited value in breast cancer prognosis [37]. Immunofluorescence staining is a relatively cumbersome procedure, still decoration of the NE would provide prognostic information, which parallel and enhance that provided by routine histological procedures.

In addition, it has been shown that doxorubicin binds first to the nuclear membrane phospholipids [38, 39] to reach its DNA target. Concurrently, Lee *et al*. [40] already demonstrated a selective binding of this drug to intranuclear tubules. It can be suggested that a marked extension of surface of contact between NE and membrane-bound chromatin, as it occurs in high NEP would result in an enhanced exposure of DNA to drugs such as anthracyclines and might provide a rational basis for tailoring treatment.

In conclusion, the present study shows that evaluation of pleomorphism of the NE represents a novel parameter of interest in pathological staging and grading.

Acknowledgements

We are grateful to Prof. Pier Carlo Marchisio, DIBIT, Department of Biological and Technological Research, San Raffaele Scientific Institute, Milano, Italy and Prof. Franco Merletti, Chair of Biostatistics, University of Turin for critically reviewing the manuscript and to Dr. Erika Ortolan, from the Department of Genetics of the Turin University for helping in the confocal microscopical study.

This work was supported by grants from AIRC (Milano, Italy), the Ministry for University (MIUR) (PRIN 2005); University of Turin (MURST ex60%); the Compagnia di San Paolo/FIRMS, Torino, Italy; Regione Piemonte 'Ricerca Scientifica Applicata' 2004 and Fondazione Cassa di Risparmio di Torino for financial support. Regione Piemonte Comitato Interministeriale per la Programmazione Economica (CIPE) 2004 provided valuable financial contributions.

References

1. **Elston CW, Ellis IO.** Pathological prognostic factors in breast cancer. I. The value of histological grade in breast cancer: experience from a large study with long-term follow-up. *Histopathology.* 1991; 19: 403–10.
2. **Volpi A, Bacci F, Paradiso A, Saragoni L, Scarpi E, Ricci M, Aldi M, Bianchi S, Muretto P, Nuzzo F, Simone G, Mangia A, Schittulli F, Amadori D.** Prognostic relevance of histological grade and its component in node-negative breast cancer patients. *Mod Pathol.* 2004; 17: 1038–44.
3. **Sloane JP, Amendoeira I, Apostolikas N, Bellocq JP, Bianchi S, Boecker W, Bussolati G, Coleman D, Connolly CE, Dervan P, Eusebi V, De Miguel C, Drijkoningen M, Elston CW, Faverley D, Gad A, Jacquemier J, Lacerda M, Martinez-Penuela J, Munt C, Peterse JL, Rank F, Sylvan M, Tsakraklides V, Zafrani B.** Consistency achieved by 23 European pathologists from 12 countries in diagnosing breast disease and reporting prognostic fea-

tures of carcinomas. European Commission Working Group on Breast Screening Pathology. *Virchows Arch.* 1999; 434: 3–10.

4. **Meyer JS, Alvarez C, Milikowski C, Olson N, Russo I, Russo J, Glass A, Zehnbauer BA, Lister K, Parwaresch R.** Cooperative Breast Cancer Tissue Resource. Breast carcinoma malignancy grading by Bloom-Richardson system vs proliferation index: reproducibility of grade and advantages of proliferation index. *Mod Pathol.* 2005; 18: 1067–78.
5. **Ghadially FN.** Ultrastructural pathology of the cell and matrix: a text and atlas of physiological and pathological alterations in the fine structure of cellular and extracellular components. 3rd ed. London: Butterworths*;* 1988; Vol. 1.
6. **Boyd J, Pienta KJ, Getzenberg RH, Coffey DS, Barrett JC.** Preneoplastic alterations in nuclear morphology that accompany loss of tumour suppressor phenotype. *J Natl Cancer Inst.* 1991; 83: 862–6.
7. **Frost JK.** The cell in health and disease: an evaluation of cellular morphologic expression of biologic behavior. 2nd rev ed. Basel: Karger*;* 1986.
8. **Fischer AH, Bond JA, Taysavang P, Battles OE, Wynford-Thomas D.** Papillary thyroid carcinoma oncogene (RET/PTC) alters the nuclear envelope and chromatin structure. *Am J Pathol.* 1998; 153: 1443–50.
9. **Fischer AH, Bardarov S Jr, Jiang Z.** Molecular aspects of diagnostic nucleolar and nuclear envelope changes in prostate cancer. *J Cell Biochem.* 2004; 91: 170–84.
10. **Fischer AH, Taysavang P, Jhiang SM.** Nuclear envelope irregularity is induced by RET/PTC during interphase. *Am J Pathol.* 2003; 163: 1091–100.
11. **Ostlund C, Worman HJ.** Nuclear envelope proteins and neuromuscular diseases. *Muscle Nerve.* 2003; 27: 393–406.
12. **Zastrow MS, Vlcek S, Wilson KL.** Proteins that bind A-type lamins: integrating isolated clues. *J Cell Sci.* 2004; 117: 979–87.
13. **Morris GE.** The role of the nuclear envelope in Emery–Dreifuss muscular dystrophy. *Trends Mol Med.* 2001; 7: 572–7.
14. **Lee KK, Haraguchi T, Lee RS, Koujin T, Hiraoka Y, Wilson KL.** Distinct functional domains in emerin bind lamin A and DNA–bridging protein BAF. *J Cell Sci.* 2001; 114: 4567–73.
15. **Wang E.** Statin, a nonproliferation-specific protein, is associated with the nuclear envelope and is heterogeneously distributed in cells leaving quiescent state. *J Cell Physiol.* 1989; 140: 418–6.
16. **Manilal S, Nguyen TM, Sewry CA, Morris GE.** The Emery-Dreifuss muscular dystrophy protein, emerin, is a nuclear membrane protein. *Hum Mol Genet.* 1996; 5: 801–8.
17. **Goldman RD, Gruenbaum Y, Moir RD, Shumaker DK, Spann TP.** Nuclear lamins: building blocks of nuclear architecture. *Genes Dev.* 2002; 16: 533–47.
18. **Gould VE, Martinez N, Orucevic A, Schneider J, Alonso A.** A novel, nuclear pore-associated, widely distributed molecule overexpressed in oncogenesis and development. *Am J Pathol.* 2000; 157: 1605–13.
19. **Fischer AH, Taysavang P, Weber CJ, Wilson KL.** Nuclear envelope organization in papillary thyroid carcinoma. *Histol Histopathol.* 2001; 16: 1–14.
20. **Papotti M, Manazza AD, Chiarle R, Bussolati G.** Confocal microscope analysis and tridimensional reconstruction of papillary thyroid carcinoma nuclei. *Virchows Arch.* 2004; 444: 350–5.
21. **Cassoni P, Marrocco T, Sapino A, Allia E, Bussolati G.** Oxytocin synthesis within the normal and neoplastic breast: first evidence of a local peptide source. *Int J Oncol.* 2006; 28: 1263–8
22. **Sapino A, Marchio C, Senetta R, Castellano I, Macrì L, Cassoni P, Ghisolfi G, Cerrato M, D'Ambrosio E, Bussolati G.** Routine assessment of prognostic factors in breast cancer using a multicore tissue microarray procedure. *Virchows Arch.* 2006; 3: 288–96.
23. European guidelines for quality assurance in breast cancer screening and diagnosis. 4th ed. C.A. Wells editors: Luxembourg, 2006.
24. **Goldberg M, Harel A., Gruenbaum Y.** The nuclear lamina: molecular organization and interaction with chromatin. *Crit Rev Eukaryot Gene Expr.* 1999; 9: 285–93.
25. **Gruenbaum Y, Wilson KL, Harel A, Goldberg M, Cohen M.** Review: nuclear lamins–structural proteins with fundamental functions. *J Struct Biol.* 2000; 129: 313–23.
26. **Nickerson J.** Experimental observations of a nuclear matrix. *J Cell Sci.* 2001; 114: 463–74.
27. **Broers JL, Hutchison CJ, Ramaekers FC.** Laminopathies. *J Pathol.* 2004; 204: 478–88.
28. **Coradeghini R, Barboro P, Rubagotti A, Boccardo F, Parodi S, Carmignani G, D'Arrigo C, Patrone E, Balbi C.** Differential expression of nuclear lamins in normal and cancerous prostate tissues. *Oncol Rep.* 2006; 15: 609–13.
29. **Dickinson HG, Bell PR.** Structures resembling nuclear pores at the orifice of nuclear invaginations in developing microspores of Pinus banksiana. *Dev Biol.* 1972; 27: 425–9.
30. **Li FL, Dickinson HG.** The structure and function of nuclear invaginations characteristic of microsporogenesis in Pinus banksiana. *Ann Bot.* 1987; 60: 321–30.
31. **Bourgeois CA, Hemon D, Bouteille M.** Structural relationship between the nucleolus and the nuclear envelope. *J Ultrastruct Res.* 1979; 68: 328–40.
32. **Dupuy-Coin AM, Moens P, Bouteille M.** Three-dimensional analysis of given cell structures: nucleo-

lus, nucleoskeleton, and nuclear inclusions. *Methods Achiev Exp Pathol.* 1986; 12: 1–25.
33. **Stevens JK, Trogadis J.** Reconstructive three-dimensional electron microscopy: a routine biological tool. *Anal Quant Cytol Histol.* 1986; 8: 102–7.
34. **Fricker M, Hollinshead M, White N, Vaux D.** Interphase nuclei of many mammalian cell types contain deep, dynamic, tubular membrane-bound invaginations of the nuclear envelope. *J Cell Biol.* 1997; 136: 531–44.
35. **Lui PP, Chan FL, Suen YK, Kwok TT, Kong SK.** The nucleus of HeLa cells contains tubular structures for Ca^{2+} signaling with the involvement of mitochondria. *Biochem Biophys Res Commun.* 2003; 308: 826–33.
36. **Kau TR, Way JC, Silver PA.** Nuclear transport and cancer: from mechanism to intervention. *Nat Rev Cancer.* 2004; 4: 106–17.
37. **Baak JP, van Diest PJ, Voorhorst FJ, Van der Wall E, Beex LV, Vermorken JB, Janssen EA.** Prospective multicenter validation of the independent prognostic value of the mitotic activity index in lymph node-negative breast cancer patients younger than 55 years. *J Clin Oncol.* 2005; 23: 5993–6001.
38. **De Wolf FA, Staffhorst RW, Smits HP, Onwezen MF, de Kruijff B.** Role of anionic phospholipids in the interaction of doxorubicin and plasma membrane vesicles: drug binding and structural consequences in bacterial systems. *Biochemistry.* 1993; 32: 6688–95.
39. **Speelmans G, Staffhorst RW, de Kruijff B, de Wolf FA.** Transport studies of doxorubicin in model membranes indicate a difference in passive diffusion across and binding at the outer and inner leaflets of the plasma membrane. *Biochemistry.* 1994; 33: 13761–8.
40. **Lee RK, Lui PP, Ngan EK, Lui JC, Suen YK, Chan F, Kong SK.** The nuclear tubular invaginations are dynamic structures inside the nucleus of HeLa cells. *Can J Physiol Pharmacol.* 2006; 84: 477–86.